The Conformations of a Functional Spin-Labeled Derivative of Gastric H/K-ATPase Investigated by EPR Spectroscopy†

David A. Middleton,‡,§ David G. Reid,|| and Anthony Watts*,‡

Department of Biochemistry, University of Oxford, Oxford OX1 3QU, U.K., and Department of Analytical Sciences, SmithKline Beecham Pharmaceuticals, Welwyn, Herts AL6 9AR, U.K.

Received September 22, 1994; Revised Manuscript Received February 7, 1995⊗

ABSTRACT: A spin-labeled derivative of porcine gastric H/K-ATPase with high ATP hydrolyzing activity (77 μmol of P_i/(mg·h)) has been prepared. Over 65% of initial ATPase activity (115 μmol of P_i/(mg·h)) was preserved after complete reaction of the enzyme with the lysine reactive nitroxide spin-labeled TEMPO isothiocyanate (TITC). In contrast, rapid and complete loss of ATPase activity occurred after reaction of the enzyme with the lysine directed fluorescent probe FITC. Conventional EPR spectra of TITC labeled H/K-ATPase reflected mainly the slow rotational diffusion of the enzyme in the membrane. An upper limit enzyme intramembranous radius of 108 Å was calculated on the basis of rotational correlation times estimated from saturation transfer (ST) EPR spectral lineshapes. Conventional EPR spectra exhibited two major components corresponding to at least two populations of strongly constrained spin-labels. Difference spectroscopy revealed that the proportion of these two components changed markedly with temperature. Moreover, the proportion of the components was sensitive to the presence of the activating ionic ligands Mg^{2+} and ATP, which induce enzyme conformational transitions, and to the reversible inhibitor SCH 28080, which binds to the K^+ sensitive form of the enzyme. These findings show that EPR spectroscopy is able to report functionally coupled conformational changes of gastric H/K-ATPase and imply that the spin-labels are attached to lysines within functionally important regions of the enzyme.

The gastric H/K-ATPase (EC 3.6.1.36) is a membrane spanning proton pump, thought to be an $\alpha\beta$ promoter, which plays a significant role in the pathogenesis of peptic ulcer disease. The enzyme is thus an important therapeutic target in biomedicinal research (Sachs et al., 1988, 1992; Rabon & Reuben, 1990). The H/K-ATPase is a member of the family of phosphorylating (P-type) ion motive enzymes, which couple ion translocation with ATP hydrolysis by means of conformational changes that alter the affinity and sidedness of ion binding (Sachs et al., 1989).

The chemomechanical coupling of structure and function by gastric H/K-ATPase has long been a subject of investigation (Helmich-de Jong et al., 1987; Jackson et al., 1983). Spectroscopic evidence for ion sensitive conformational states of the H/K-ATPase and Na/K-ATPase has been gained from fluorimetric studies of the enzymes after modification with the covalently reacting label fluorescein 5′-isothiocyanate (FITC)[1] (Jackson et al., 1983; Faller et al., 1991). FITC reacts exclusively with a specific lysine residue within a conserved pentapeptide region of the P-type ATPases. Reaction with FITC is accompanied by a rapid loss of ATP hydrolytic activity (Farley & Faller, 1985; Faller et al., 1991), but ion sensitivity and the ability of these enzymes to hydrolyze *p*-nitrophenyl phosphate (pNPP) are unaffected (Jackson et al., 1983). The ionic ligands K^+, Na^+, and Mg^{2+} induce changes in fluorescence of FITC modified H/K-ATPase and Na/K-ATPase, which are believed to represent conformational transitions of these enzymes between E_1 (ATP binding) and E_2 (K^+ sensitive) forms (Jackson et al., 1983; Faller et al., 1991). ATP protects against both FITC inactivation and incorporation of the label into these enzymes, from which it was inferred that the conserved region is close to the site that binds the adenine ring of ATP (Jackson et al., 1983; Karlish, 1980).

There is some evidence that ion and substrate induced conformational changes of the P-type ATPases involve alterations in local and global enzyme mobility (Esmann, 1982; Hidalgo et al., 1978). Both conventional and saturation transfer electron paramagnetic resonance (EPR) spectroscopy have been demonstrated to be powerful methods for probing the dynamics of the Na/K-ATPase and the Ca/Mg-ATPase after incorporation of nitroxide spin-labels into the enzymes as probes of their mobilities within the membrane (Thomas & Hidalgo, 1978; Esmann et al., 1987, 1992). Conventional EPR spectra of *Squalus acanthias* Na/K-ATPase, after spin-labeling of enzyme sulfhydryl groups, exhibited two components representing spin-labels either weakly or strongly constrained at their points of covalent attachment to the enzyme (Esmann, 1982). The proportions of weakly and strongly immobilized labels were sensitive to the presence of activating cations Na^+ and K^+. The global rotational mobility of large proteins within membranes has been probed using saturation transfer (ST) EPR spectroscopy, a technique that is sensitive to motions with correlation times of between 10^{-7} and 10^{-2} s (Thomas et al., 1976; Horváth & Marsh, 1983, 1988). The rotational diffusion of Ca/Mg-ATPase and

† This work was supported in part by the Science and Engineering Research Council (CASE studentship to D.A.M.).

* Author to whom correspondence should be addressed.

‡ University of Oxford.

§ Present address: Department of Analytical Sciences, SmithKline Beecham Pharmaceuticals, Welwyn, Herts AL6 9AR, U.K.

|| SmithKline Beecham Pharmaceuticals.

⊗ Abstract published in *Advance ACS Abstracts,* May 15, 1995.

[1] Abbreviations: EPR, electron paramagnetic resonance; STEPR, saturation transfer EPR; TITC, TEMPO isothiocyanate; FITC, fluorescein isothiocyanate; P_i, inorganic phosphate.

0006-2960/95/0434-7420$09.00/0

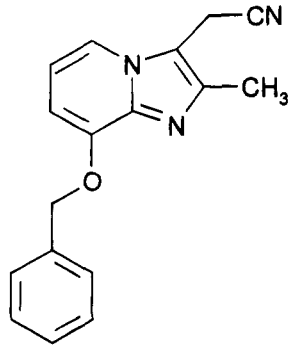

FIGURE 1: Chemical structure of the K^+ competitive, reversible H/K-ATPase inhibitor, SCH 28080.

Na/K-ATPase under various conditions have been examined extensively using STEPR (Thomas & Hidalgo, 1978; Karon & Thomas, 1993; Esmann et al., 1987, 1994).

The aim of this work was to gain insight into the conformational changes and concomitant rotational mobility of gastric H/K-ATPase during the phosphoenzyme cycle. Clearly, it was necessary to use a technique that was informative without perturbing enzyme functionality. EPR spectroscopy was the method of choice as we were able to incorporate nitroxide spin-labels (TEMPO isothiocyanate; TITC) into the H/K-ATPase with only a small perturbation of ATPase activity. Here, we characterize the activity of the spin-labeled enzyme and compare it with that of FITC modified enzyme. It is demonstrated that known functionally coupled conformational changes of the spin-labeled enzyme, induced by Mg^{2+} and ATP, are accompanied by measurable changes in the lineshape of the EPR spectrum. It is also shown that the EPR spectrum is sensitive to the addition of a reversible inhibitor, SCH 28080 (Figure 1), to the enzyme in the presence of ATP. SCH 28080 binds noncovalently to the E_2 (K^+ sensitive) form of both phosphorylated (E_2P) and nonphosphorylated H/K-ATPase at the extracytoplasmic face (Mendlein & Sachs, 1990; Keeling et al., 1989). We attempt to rationalize the observed spectral changes in terms of different enzyme conformational states by examining temperature, ligand, and inhibitor dependent changes in spin-label dynamics.

MATERIALS AND METHODS

Enzyme Preparation. H/K-ATPase was isolated in microsomal membranes from hog stomachs by differential centrifugation of homogenized fundic scrapings (60 g) using a method similar to that described in detail elsewhere (Swarts et al., 1991). Further purification of H/K-ATPase was achieved by layering the microsomes onto a gradient of 9.5% (w/v) Ficoll in 0.25 M sucrose and 30% sucrose in 5 mM Tris-HCl (pH 7.4) followed by centrifugation at 100000*g* for 90 min. The H/K-ATPase enriched microsomes were harvested from the 0.25 M sucrose−9.5% (w/v) Ficoll in 0.25 M sucrose interface. Sucrose was removed by three washing cycles of centrifugation at 100000*g* and suspension in 5 mM Tris-HCl containing 1 mM EDTA. The microsomes were lyophilized overnight and resuspended in 40 mM Tris-HCl (pH 7.4) and stored at 4 °C.

Purity of H/K-ATPase Preparation. It was essential to obtain a high purity enzyme preparation for modification with spin-label, to avoid excessive labeling of protein contaminants which could contribute to the EPR spectral intensity. The purity of H/K-ATPase in the microsomes was ascertained by measurement of K^+ stimulated activity and estimation of protein composition by SDS-PAGE. The K^+ stimulated ATPase activity of lyophilized microsomes at 37 °C, quantified as P_i liberated per milligram of protein in a standard reaction medium (Saccomani et al., 1977), was 80−110 μmol of P_i/(mg·h). This activity was comparable to activities for preparations obtained previously, in which the H/K-ATPase α subunit, migrating at ca. 94 kDa on SDS−polyacrylamide gels, was estimated to represent 75% of total protein by densitometric analysis of the gels (Saccomani et al., 1977; Chang et al., 1979). In the present work, Coomassie Blue stained SDS gels of microsomes exhibited a major band at 94−104 kDa accounting for 80% of the dye absorbance. Much of the remaining absorbance was located in the 60−80 kDa range (where the H/K-ATPaes β subunit migrates), with less than 10% of absorbance being from unidentified contaminants.

A further issue regarding purity is that of basal Mg^{2+}-ATPase activity. This partial reaction, present in all preparations of the enzyme, is thought not to be linked to ion transport. Mg^{2+} dependent activity could arise from spontaneous, unstimulated dissociation of the phosphoenzyme implicated in the H/K-ATPase catalytic cycle, or from a separate phosphatase reaction by an impurity in the preparation (Wallmark et al., 1987; Van der Hijden, 1990). The reversible H/K-ATPase inhibitor SCH 28080 (Figure 1) inhibits K^+ stimulated ATPase activity (K_i = 66 nM at pH 7.4) and up to 70% of the basal Mg^{2+} ATPase activity in gastric microsomes (Keeling et al., 1988; Wallmark et al., 1987). In the present work, only 20% of initial Mg^{2+} ATPase (7.8 ± 2.5 μmole/(mg·h)) was inhibited by 1 mM SCH 28080. The residual Mg^{2+}-ATPase activity could in principle represent enzyme contaminants in the microsome preparation.

Derivatization of H/K-ATPase. Lyophilized microsomes containing 2 mg of protein were suspended in a total volume of 1 mL of reaction buffer (40 mM Tris-HCl, pH 8.2). The suspension was made 0.15 mM in either the spin-label TEMPO isothiocyanate (TITC) or the fluorescent label FITC (both obtained from Sigma Chemical Co., U.K.) by addition of the labeling reagent in 10 μL of DMSO from a stock solution of 15 mM, followed by gentle stirring of the suspension at 20 °C for 1−2.5 h. The reaction was quenched by addition of 5 mL of ice-cold buffer (40 mM Tris-HCl, pH 8.2), and unreacted label was removed by several cycles of centrifugation at 100000*g* and resuspension in 1 mL of 40 mM Tris-HCl, pH 8.2. For TITC labeling, a small remaining amount of unreacted label was removed by stirring the microsomes with nonpolar absorbent polystyrene beads (Bio-Beads SM-2, Bio-Rad) at 20 °C for 30 min. Prolonged exposure of microsomes to the beads did not affect enzyme activity, but some loss of protein was observed after 1 h incubation, presumably because of adsorption to the beads. The microsomes were separated from the bead suspension by elution from a plastic syringe barrel subjected to centrifugation (3000 rpm; 5 min). The final stoichiometry of binding of TITC to H/K-ATPase was estimated spectroscopically from standard EPR integrals. Briefly, conventional EPR spectra of a series of concentrations of TITC in water (1 nM−1 mM) were recorded at 0 °C, under the same conditions and with the same receiver gain and the same number of scans as for spectroscopy of H/K-ATPase.

Calibrations were constructed from the conventional EPR double integral at each concentration of aqueous TITC. The TITC−H/K-ATPase binding stoichiometry was determined by interpolation of the double integrals of H/K-ATPase spectra and (Lowry) quantitation of the protein content of the EPR capillary tube. The FITC binding stoichiometry was measured after SDS solubilization of the microsomes as described elsewhere (Jackson et al., 1983).

Electron Spin Resonance. EPR spectra were recorded at 9.5 GHz on a Bruker ESP 300 spectrometer equipped with ESP 1600 data station and variable temperature controller regulated by nitrogen gas flow. Membrane samples were contained in 1 mm internal diameter glass capillary tubes sealed at one end and placed within a 4 mm quartz NMR tube. Sample volumes were adjusted to occupy 5 mm of the capillary tube, and samples were positioned centrally within the microwave cavity. Conventional in-phase first harmonic EPR spectra (V_1 display) were recorded at a nonsaturating microwave power of 10 mW with a field modulation frequency of 100 kHz and modulation amplitude of 0.1 mT peak-to-peak. Saturation transfer EPR spectra were recorded 90° out-of-phase in the second harmonic absorption mode (V_2' display) at a modulation frequency of 50 kHz and a modulation amplitude of 0.5 mT peak-to-peak (Hemminga et al., 1984). The microwave power was adjusted to give an average field strength over the sample of $\langle H_1^2 \rangle^{1/2} = 2.5 \times 10^{-2}$ mT, calibrated using 1 mM PADS in deoxygenated K_2CO_3 (Hemminga & De Jager, 1989).

Calculation of Rotational Correlation Times. Correlation times for effective isotropic rotational diffusion of H/K-ATPase in the lipid bilayer, τ_R^{eff}, were estimated from STEPR spectral lineheight ratios in the low-field (L''/L) and high-field (H''/H) regions (Thomas et al., 1976) using calibration curves for spin-labeled hemoglobin (Horváth & Marsh, 1983, 1988). A more appropriate measure of the anisotropic rotation of the protein in the membrane is given by the uniaxial correlation time, $\tau_{R\parallel}$, related to the effective correlation time by (Esmann et al., 1987)

$$\tau_{R\parallel} = 1/(6D_{R\parallel}) = (0.5)\tau_R^{eff} \sin^2 \theta \qquad (1)$$

where $D_{R\parallel}$ is the rotational diffusion coefficient of the protein and θ is the orientation of the spin label z axis relative to axis of protein rotation (the membrane normal). An upper limit for the uniaxial rotational correlation time of the protein is given assuming $\theta = 90°$; i.e.,

$$\tau_{R\parallel} = (0.5)\tau_R^{eff} \qquad (2)$$

RESULTS AND DISCUSSION

Functional Characterization of Modified H/K-ATPase. Ouabain insensitive Mg^{2+} dependent and K^+ stimulated ATPase activities of lyophilized, H/K-ATPase enriched microsomes were measured at defined time intervals over a 2 h period in the presence of either 0.15 mM TITC or 0.15 mM FITC. Both labels have the isothiocyanato functionality, which is highly reactive toward accessible lysine residues. The time courses of ATPase activity in the presence of labeling reagents were measured over a 2 h period (Figure 2). Minimal loss of H/K-ATPase activity in the control medium containing DMSO occurred over this time. In the presence of TITC or FITC, however, Mg^{2+} dependent and K^+ stimulated activities decreased in the first 30 min of incubation. The time course of FITC inactivation agreed with previous findings (Jackson et al., 1983). Little or no further reduction in activity occurred after 30 min of incubation with either reagent. Residual K^+ stimulated activities of microsomes after 2 h incubation were ca. 65% of control in the presence of TITC and ca. 10% in the presence of FITC. Mg^{2+} dependent activity was reduced in similar proportion to H/K-ATPase activity in both cases. The control K^+ stimulated ATPase activity (in the absence of either label) was 103 ± 20 μmol/(mg·h) at pH 8.2. Raising the pH of the incubation medium to 9.2, for consistency with the FITC labeling procedure of Jackson et al. (1983), reduced the control K^+ stimulated activity to below 80 μmol/(mg·h). The extent and time course of enzyme inactivation by TITC and FITC at pH 9.2 did not differ from that at pH 8.2 when expressed relative to control measurements.

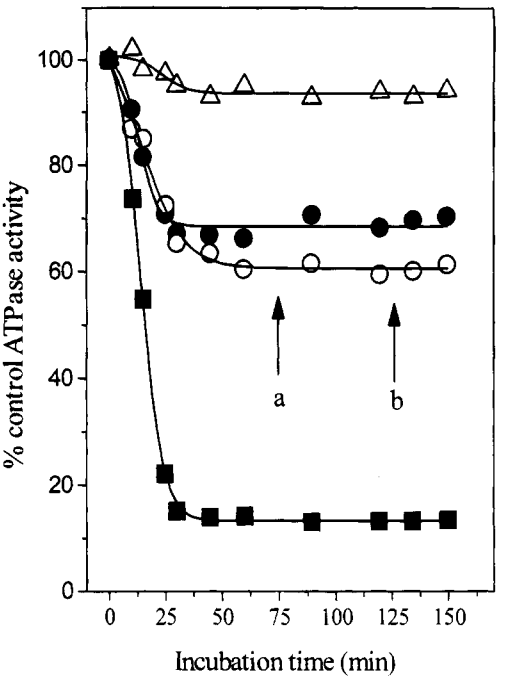

FIGURE 2: Time course of Mg^{2+} dependent and K^+ stimulated ATP hydrolysis by gastric H/K-ATPase in lyophilized microsomes at 37 °C. K^+ stimulated ATPase activity was measured with either 5 μL of DMSO (△), 0.15 mM TITC (●), or 0.15 mM FITC (■) in the assay medium. Arrow "a" indicates the time at which a further 0.15 mM TITC was added to the assay mixture containing TITC treated microsomes. Arrow "b" signifies the time at which 0.15 mM FITC was added to the TITC pretreated microsomes. Mg^{2+} dependent activity of microsomes was measured in the presence of 0.15 mM TITC as the only labeling reagent (○).

It was important to establish whether the 35% reduction of control enzyme activity by TITC arose from a uniform reduction in the rate of hydrolysis throughout the H/K-ATPase population rather than, for instance, a complete inhibition of 35% of the enzyme because of heterogeneous labeling. A second addition of 0.15 mM TITC to the microsomes after 2 h prior incubation with TITC (Figure 2, arrow "a") did not reduce H/K-ATPase activity further. This confirmed that all sites available for modification had reacted with the label and implied that labeling was homogeneous throughout the enzyme population. Preservation of hydrolytic activity after TITC labeling, rather than inactivation seen after FITC labeling, suggested that the relative sizes of the two probes imposed different extents of perturbation or that TITC did not react with the site of inactivation by FITC.

Table 1: Kinetic Parameters for ATPase Activity of Gastric H/K-ATPase Labeled with TITC and FITC[a]

label	V_{max} (μmol/(mg·h)[b] Mg^{2+}	V_{max} (μmol/(mg·h)[b] K^+	K_m (mM)[b] K^+
control	8.3	115	1.20
TITC	5.5	77	1.32
FITC	<1	10	

[a] Microsomes were incubated with DMSO (control), TITC, or FITC at 20 °C for 1 h. Activity was quantified as inorganic phosphate (P_i) liberated as described in Materials and Methods. [b] The ATP concentration was constant at 2 mM, and the KCl concentration was varied between 0.1 and 50 mM.

Table 2: Stoichiometries of Reaction of TITC and FITC with Microsomal Gastric H/K-ATPase[a]

label	amt reacted (nmol/mg)
0.15 mM FITC[b]	1.8 ± 0.3 (4)
0.15 mM TITC[b]	4.5 ± 0.5 (4)
0.15 mM FITC + 0.15 mM TITC[c]	2.5 ± 0.3 (3)
0.15 mM TITC + 0.15 mM FITC[d]	0 (3)

[a] Lyophilized microsomes containing 1 mg (Lowry) of protein were incubated for up to 90 min in 1 mL of 40 mM Tris-HCl, pH 8.2 at 20 °C, in the presence of covalently reacting label. Numbers of individual measurements are given in parentheses. [b] Reaction was quenched after 40 min by addition of ice-cold lysine. [c] TITC was added after 40 min prior incubation with FITC and reaction was quenched after a further 40 min. [d] FITC was added after 40 min prior incubation with TITC and reaction was quenched after a further 40 min.

When TITC was incubated with microsomes prior to addition of FITC (Figure 2, arrow "b"), the spin-label protected against FITC inactivation, as evidenced by the minimal effect of the fluorescent probe on the residual Mg^{2+} dependent or K^+ stimulated activity. It is likely, therefore, that TITC either sterically hindered FITC from reacting with the site of inactivation or had itself already reacted with this site.

The maximal Mg^{2+} dependent ATPase activity (V_{max}) of the microsomes was reduced by TITC to the same extent (65% of initial activity) and at the same rate (Figure 2) as the maximal K^+ stimulated ATPase activity (Table 1). The parallel reduction in activities suggested that Mg^{2+}- and K^+-ATPase activities were coupled and hence that basal Mg^{2+}-ATPase activity did not arise wholly from an independent enzyme contaminant. K^+ stimulated ATP hydrolysis (in the presence of Mg^{2+}) by both native and spin-labeled enzyme obeyed Michaelis–Menten kinetics. The K_m for K^+ stimulated inorganic phosphate liberation increased from 1.20 mM to 1.32 mM after TITC labeling of the enzyme. This small increase could represent hindrance of phosphorylation, dephosphorylation, or K^+ binding by the spin-label. The concomitant reduction in the rate of Mg^{2+}-ATPase activity by TITC labeling suggested that interaction of the label with the reaction cycle occurred at the cytoplasmic face of the enzyme. Nevertheless, the reaction cycle of H/K-ATPase is complex, and K_m values based on rates of ion stimulated hydrolysis cannot be interpreted unambiguously as interference of the label with a single step of the cycle.

The stoichiometry of reaction of FITC after maximum inactivation was estimated to be 1.8 nmol/mg of protein (Table 2), which agreed closely with previous data and is the approximate stoichiometry of phosphorylation by ATP (1.5 nmol/mg); i.e., 1 FITC label reacts per phosphorylation site (Jackson et al., 1983). The TITC reaction stoichiometry was estimated to be ca. 5–6 nmol/mg of protein, indicating a lower selectivity of reaction compared with FITC. This indicated that a greater number of reactive sites were accessible to the spin-label than to the fluorescent probe, possibly in the large cytoplasmic domain of the enzyme. The stoichiometry of TITC labeling was reduced to ca. 3–4 nmol/mg of protein when microsomes were first labeled with FITC, indicating that the fluorescent label partially protected spin-labeling of the enzyme. It is unlikely that the high reaction stoichiometry of TITC represented a significant labeling of non-ATPase impurities, since these were estimated to represent less than 10% of the protein composition of the membrane.

Conventional EPR Spectra of TITC Labeled H/K-ATPase. Enzyme was spin-labeled at room temperature by incubation of lyophilized, resuspended microsomes with TITC for 1 h. Small amounts of unreacted spin-labeled were removed only after repeated washing of the sample followed by treatment with nonpolar absorbent beads. The small residual unreacted TITC present after washing may have been bound noncovalently to the microsomes, since adsorption of the spin-label to the beads was necessary for its removal. Ionic ligands were added to the spin-labeled H/K-ATPase to investigate whether the EPR lineshape was sensitive to different functional states of the enzyme over a 0–25 °C temperature range (Figure 3). Spectra of nonfunctional enzyme (i.e., in the absence of ATP) were recorded in the presence of either 2 mM Mg^{2+} (Figure 3A) or EDTA (not shown), to examine whether any lineshape changes were caused by a transition of the enzyme to a divalent metal ion sensitive conformer. Conformational changes accompanying Mg^{2+} dependent phosphorylation and unstimulated dephosphorylation of the enzyme were investigated by addition of 2 mM ATP and 2 mM Mg^{2+} to the microsomes immediately before recording of spectra (Figure 3B). The effect of inhibitor binding was investigated by addition of 1 mM SCH 28080 to enzyme in the presence of 2 mM Mg^{2+} and 2 mM ATP (Figure 3C).

Conventional EPR spectra of the spin-labeled preparations exhibited an outer component corresponding to strongly constrained spin-label (denoted "S" in Figure 3) and representing >95% of integrated intensity. A minor (<5%) component from weakly constrained label (denoted "W" in Figure 3) was also in evidence. These spectra reflected chiefly the rotational motions of the enzyme occurring on a time scale (correlation time $\tau_c < 10^{-7}$ s) slower than that of conventional EPR spectroscopy. In each case, close examination of the high-field extremum of the outer component revealed a somewhat asymmetric lineshape (expanded for clarity in Figure 3A–C). This feature appeared to arise from two overlapping components separated by several gauss (labeled "S1" and "S2" in Figure 3) and indicated different populations of strongly constrained spin-labels. The high-field extrema of the spectra could be simulated convincingly by least-squares fitting of double Gaussian curves to the experimental data, from which were obtained estimates of the relative maxima of the two overlapping high-field components, S1 and S2 (Figure 4). In contrast, the low-field extrema of the spectra did not exhibit well-defined separate components; without deconvolution only a single maximum could be measured with certainty.

For enzyme in the presence of Mg^{2+}, systematic changes in the lineshapes of the outer extrema were observed as the temperature was raised from 0 to 25 °C (Figure 4). Virtually

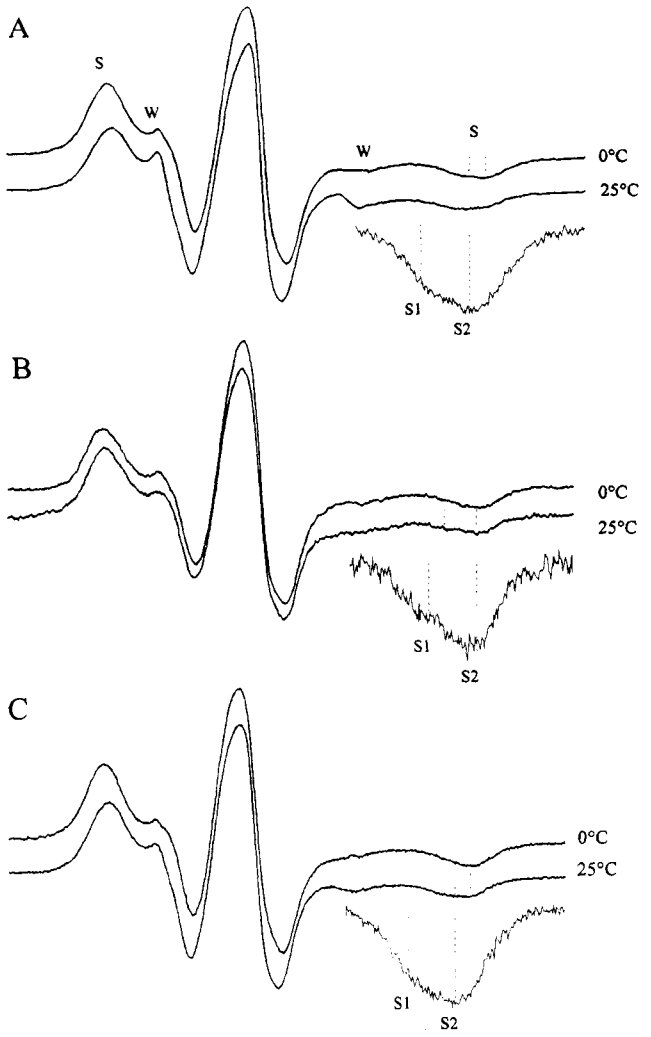

FIGURE 3: Conventional EPR spectra (V_1 display) of H/K-ATPase in gastric microsomes, after incubation with 0.15 mM TITC for 1 h. Unreacted spin-label was removed as described in text. The enzyme suspension medium contained either $MgSO_4$ (A), 2 mM $MgSO_4$ and 2 mM ATP (B), or 2 mM $MgSO_4$, 2 mM ATP, and 1 mM SCH 28080 (C). Spectra exhibited a major outer component from strongly constrained spin-labels ("S") and a small inner component from weakly constrained labels ("W"). The high-field extremum of the outer component (expanded for clarity) appeared to consist of two overlapping components, which we have denoted "S1" and "S2". Total scan width 100 G.

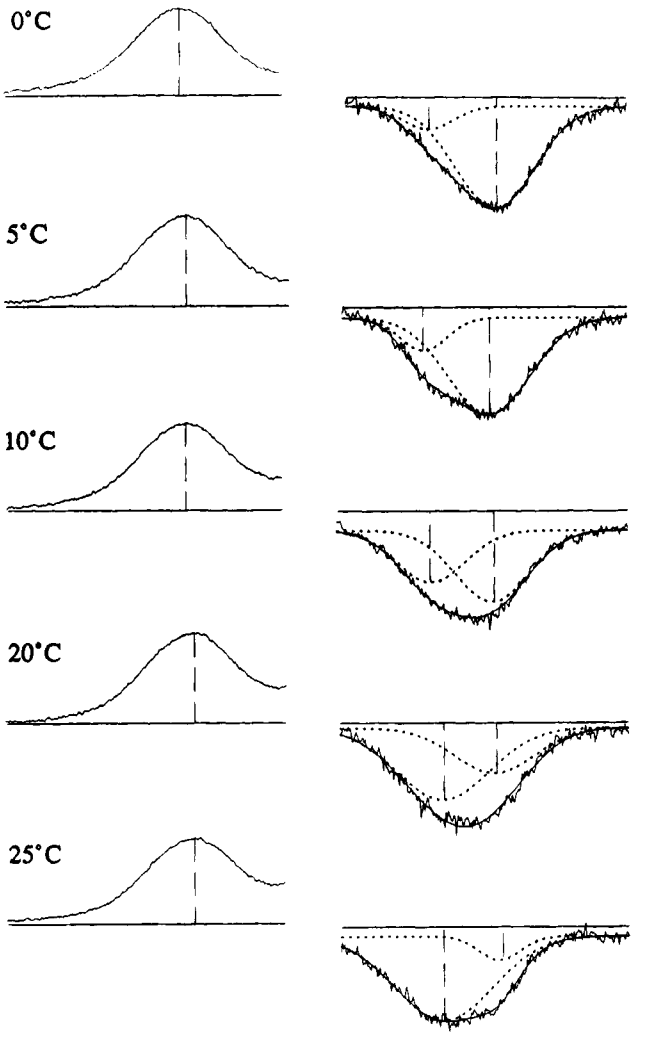

FIGURE 4: Temperature dependence of the EPR outer extrema for TITC labeled H/K-ATPase in the presence of 2 mM $MgSO_4$. The high-field extrema are simulated using a double Gaussian function (solid line) and shown with the individual simulated components (dotted lines). Peak maxima at each temperature are illustrated by the dashed lines.

identical changes were observed for enzyme in the presence of EDTA and hence are not shown. Lineshape simulations suggested slight changes in the field positions of the high-field (S1 and S2) and low-field extrema. More interestingly, the relative intensities of S1 and S2 appeared to change progressively with temperature (Figure 4). Analysis of high-field extrema for enzyme in the presence of Mg^{2+}, ATP, and SCH 28080 revealed similar trends over this temperature range.

Dual Component Lineshape Analysis. In order to gain a more accurate impression of the proportions of the two spectral components, S1 and S2, it was necessary to deconvolute the components using difference spectroscopy (Figure 5). In this way, the double integrals of the difference spectra, being related to spin concentration, could be taken as a measure of the relative proportions of the two distinct spin-label populations.

Suitable model spectra were chosen to represent the outermost (S2) component of the enzyme spectrum at each temperature. Model spectra were obtained at suitable temperatures from TITC reacted with a single primary amine group of an immobilizing support. A starting point for obtaining the most suitable model spectrum of the right intensity for subtraction was a close fit of the model high-field extremum to the Gaussian simulation of the enzyme spectrum high-field S2 extremum (Figure 5B). Slight adjustments in the proportion of the subtracting model spectrum were then necessary, so that a difference spectrum of appropriate lineshape was obtained, corresponding to the inner S1 component (Figure 5C). The model spectrum was taken to represent the outer S2 component. The proportions of the spin populations giving rise to S1 and S2 were calculated from double integrals of the difference spectra and model spectra, respectively. Absolute spin-label concentration at each temperature was not determined, but double integrals of the dual component spectra were found not to diminish appreciably at higher temperatures.

Deconvolution of the two spectral components, S1 and S2, for all the enzyme spectra, was made possible by the

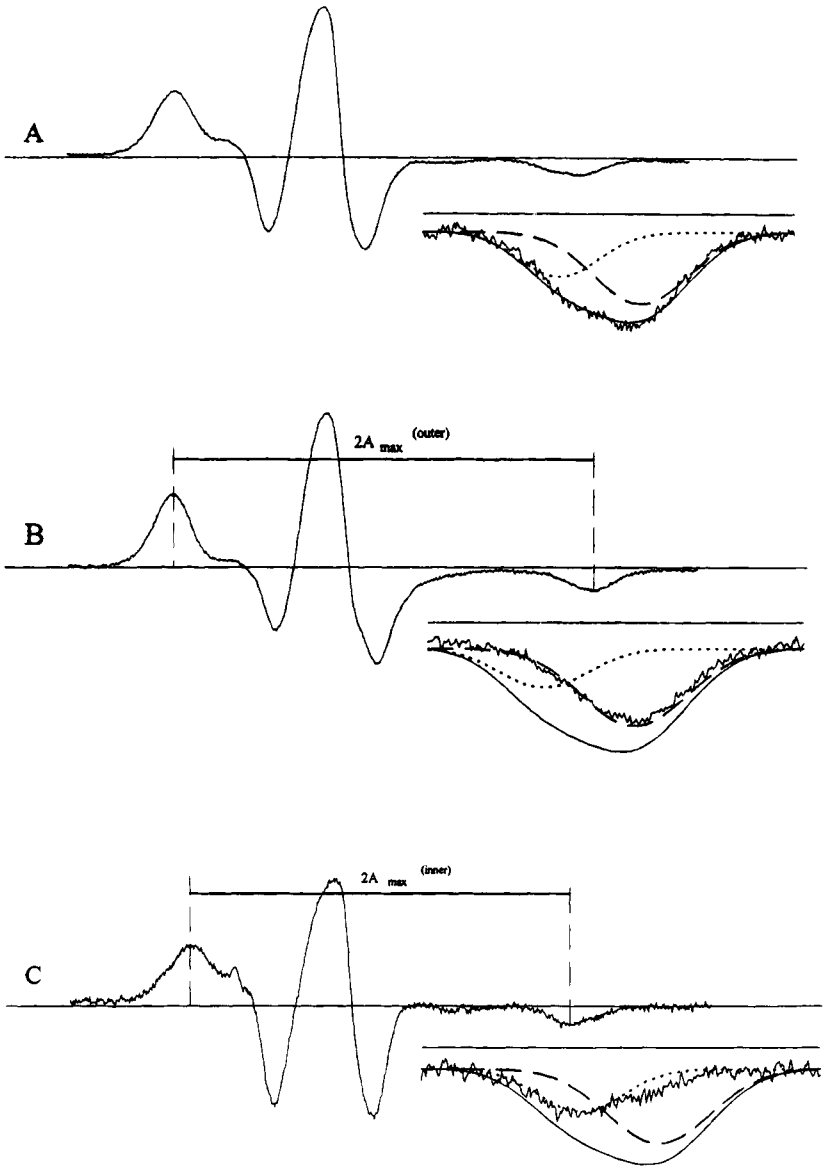

FIGURE 5: Illustration of the technique for deconvolution of conventional EPR spectra of H/K-ATPase labeled with TITC. (A) Spectrum of enzyme in the presence of $MgSO_4$, with Gaussian simulation of the high-field extremum (see Figure 4); (B) a suitable model spectrum was chosen to represent the outermost (S2) component of the enzyme spectrum; the proportion (68%) and outer hyperfine splitting ($2A_{max}$) of the model spectrum were such that the model high-field extremum fitted closely to the corresponding single component Gaussian simulation of the enzyme spectrum (dashed line); (C) difference spectrum, representing 32% of original spectral intensity, obtained by subtraction of the model spectrum from the spectrum of TITC labeled H/K-ATPase. Note the superposition of the difference spectrum outer extremum and the corresponding single Gaussian simulation of the enzyme spectrum (dotted line).

significant difference in their outer hyperfine splittings, $2A_{max}$ (e.g., see Figure 5). The outer hyperfine splitting for strongly constrained spin-labels is a measure of the residual mobility of the labels on the conventional EPR time scale, according to the deviation of this parameter from the rigid limit value, $2A_{zz}$ (67.5 G, measured from the model spectrum at −50 °C). Values of $2A_{max}$ of around 59 and 67 G were measured at 0 °C for the inner (S1) and outer (S2) component, respectively. The lower of the two values decreased slightly as the temperature was raised (Table 3), probably a corollary of some residual motion of the spin-labels on the millisecond time scale. Residual spin-label mobility in various derivatives of *Squalus* Na/K-ATPase was proposed to originate from segmental motions of the labels relative to the enzyme (Esmann et al., 1992). Here, the difference in $2A_{max}$ for the two spectral components S1 and S2 (almost 10 G) suggests a large disctinction in the rates of motion of the two populations of spin-label. It is envisaged, therefore, that the outer component (S2) probably arises from strongly constrained spin-labels in a virtually rigid environment whereas the inner component (S1) is from labels in a less constrained environment.

Ionic Ligand Dependent Changes in Spin-Label Populations. Difference spectroscopy permitted estimations to be made of the proportions of the two constrained spin-label populations, and changes therein at different temperatures and in the presence of ionic ligands (Figure 6).

The spectra of enzyme in the presence of either EDTA or Mg^{2+} exhibited similar, but pronounced, changes with temperature. The inner (S1) spectral component intensified progressively relative to the outer component, accounting for ca. 16% of overall signal at 0 °C and ca. 80% of signal at 25 °C (Table 3). The two spectral components perhaps represented different structural states of the enzyme in

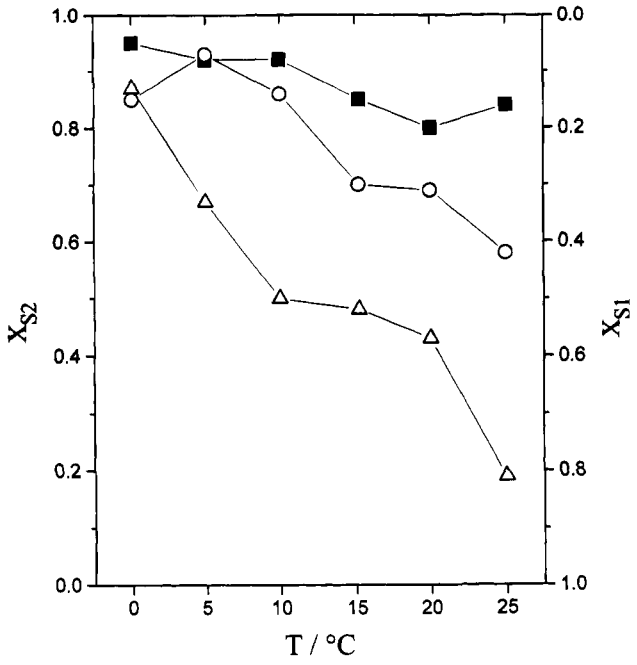

FIGURE 6: Variation with temperature of the proportions (X) of the inner (S1) and outer (S2) components of conventional EPR spectra of TITC labeled H/K-ATPase in a suspension medium containing either 2 mM Mg^{2+} (△), 2 mM $MgSO_4$ and 2 mM ATP (■), or 2 mM $MgSO_4$, 2 mM ATP, and 1 mM SCH 28080 (○). The two components S1 and S2 were assumed to represent 100% of the spectral intensity for strongly constrained spin-labels.

Table 3: Estimates of the Proportions of the Inner (S1) and Outer (S2) Components in EPR Spectra of Gastric H/K-ATPase Labeled at Lysine Residues with TITC[a]

		inner (S1)		outer (S2)	
enzyme medium	T (°C)	$2A_{max}$[b] (G)	X_{S1}	$2A_{max}$[c] (G)	X_{S2}[d]
1 mM EDTA	0	59.4	0.16	67.3	0.84
	25	59.1	0.80	67.4	0.20
2 mM Mg^{2+}	0	59.27	0.11	67.5	0.89
	25	59.16	0.84	67.3	0.16
2 mM Mg^{2+}/2 mM ATP	0	59.8	0.05	67.5	0.95
	25	58.5	0.20	67.2	0.80
1 mM SCH 28080	0	58.8	0.15	67.3	0.85
	25	58.3	0.43	67.5	0.57

[a] Suitable model EPR spectra approximating to the outer (S2) component were subtracted from the enzyme spectra in suitable proportion to leave by difference the spectra of the inner (S1) component (Figure 5). [b] The inner hyperfine splitting, $2A_{max}$, was measured from the initial model spectra used for subtraction. [c] The outer hyperfine splitting, $2A_{max}$, was measured from the resulting difference spectra. [d] The proportion of the two components, X_{S1} and X_{S2}, was determined from the double integrals of the dual component and difference spectra, respectively.

dynamic equilibrium (but in slow exchange on the EPR time scale). The change in their proportions might indicate a shift in the equilibrium in favor of one or more of these conformers at higher temperature, thus altering the motional environment of the spin-labels from a rigid state to more mobile state. Previous work, using trypsin digest and fluorimetric methods, has provided evidence for a Mg^{2+} sensitive conformer of gastric H/K-ATPase (Helmich-de Jong et al., 1986, 1987). Here, EPR difference spectroscopy could not distinguish between a putative Mg^{2+} sensitive form and the form(s) of the enzyme in the absence of divalent cations (i.e., in the presence of EDTA). Rather, the observed change in spectral proportions occurred independent of ionic ligands. Inhibitor binding studies indicate that the nonphosphorylated enzyme exists in both E_1 (Mg^{2+} and ATP sensitive) and E_2 (K^+ and SCH 28080 sensitive) forms (Sachs & Mendlein, 1990; Keeling et al., 1989). It is possible that our findings represent transitions between these two forms.

Spectra of H/K-ATPase in the presence of Mg^{2+} and ATP also indicated an increasing relative intensity of the S1 component (decrease of the S2 component) as the temperature was raised (Figure 6). At 25 °C in the presence of these ligands, the S1 component represented 16% of total intensity, compared to 80% seen in the presence of EDTA or Mg^{2+} alone (Table 3). The addition of ATP therefore appeared to impede the transition of spin-labels from one environment to the other, thus allowing a spectroscopic distinction to be made between enzyme in the presence and in the absence of nucleotide. Enzyme conformational transitions are thought to be induced after phosphorylation by ATP, viz., $E_1 \rightleftharpoons E_1P \rightleftharpoons E_2P$ (Wallmark et al., 1980; Helmich-de Jong et al., 1987). Such transitions could shift the dynamic equilibrium away from the enzyme state that predominates at high temperature in the absence of nucleotide, in this case, away from the state associated with the less constrained spin-labels, toward the state associated with more rigid labels.

The substituted imidazo[1,2-*a*]pyridine SCH 28080 (Figure 1) binds predominantly to the E_2P form of gastric H/K-ATPase with high affinity, preventing stimulated dissociation of the phospho intermediate and thereby inhibiting ion translocation (Wallmark et al., 1987; Keeling et al., 1989). As in the cases described above, a progressive increase with temperature in the intensity of the inner S1 component was seen in spectra of enzyme in the presence of Mg^{2+}, ATP, and 1 mM SCH 28080 (Figure 6). At 25 °C, the S1 component accounted for 40% of overall spectral intensity (Table 3), hence being of greater proportion than observed in the presence of Mg^{2+} and ATP alone (16%), but of somewhat smaller proportion than in the absence of all ionic ligands (80%). Binding of SCH 28080 to the E_2P form (and, to a lesser extent, the nonphosphorylated E_2 form) might stabilize the enzyme in these forms by slowing down or inhibiting subsequent steps of the ATPase reaction cycle. Since the inner S1 component (from less constrained spin-labels) for phosphorylated enzyme at 25 °C was comparatively more intense in the presence of SCH 28080 than in the absence of the inhibitor, it is conceivable that the less constrained spin-labels are associated with the stabilized E_2 or E_2P forms.

Rotational Correlation Times of H/K-ATPase. Spin-labels were found to be fully immobilized, or highly constrained on the conventional EPR time scale. Motions of $\tau_c < 10^{-7}$ s are accessible to STEPR spectroscopy; thus the slow rotational diffusive motions of spin-labeled H/K-ATPase were examined quantitatively by this technique. STEPR spectra (V_2' display) were recorded of enzyme in the presence of EDTA, or the ionic ligands Mg^{2+} and ATP in the absence or presence of SCH 28080, over a 0−25 °C temperature range, i.e., under the same conditions as for the conventional spectra (Figure 7). Enzyme rotational correlation times were estimated from the lineheight ratios in the high-field and low-field regions, L''/L and H''/H, respectively (defined by Thomas et al., 1976; see Figure 7a for details of measurement) and from normalized spectral integrals, I_{ST} (Horváth & Marsh, 1983, 1988). Spectra were not distorted ap-

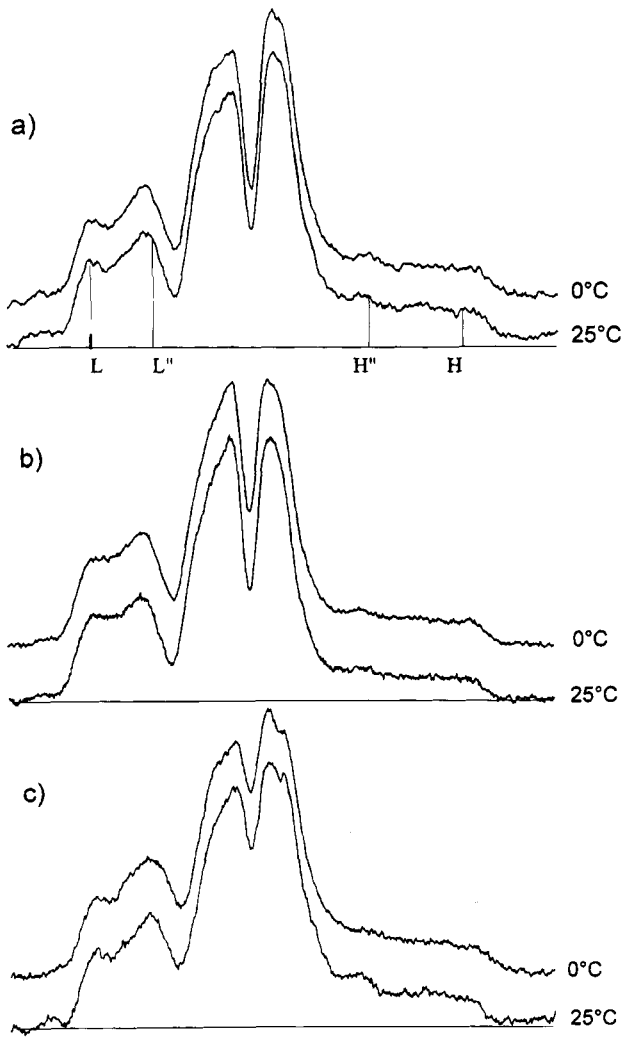

FIGURE 7: Second harmonic, 90° out-of-phase STEPR spectra (V_2' display) of H/K-ATPase in gastric microsomes, after incubation with 0.15 mM TITC for 1 h. Unreacted spin-label was removed as described in the text. The enzyme suspension medium contained either 1 mM EDTA (a), 2 mM $MgSO_4$ and 2 mM ATP (b), or 2 mM $MgSO_4$, 2 mM ATP, and 1 mM SCH 28080 (c). Total scan width 100 G.

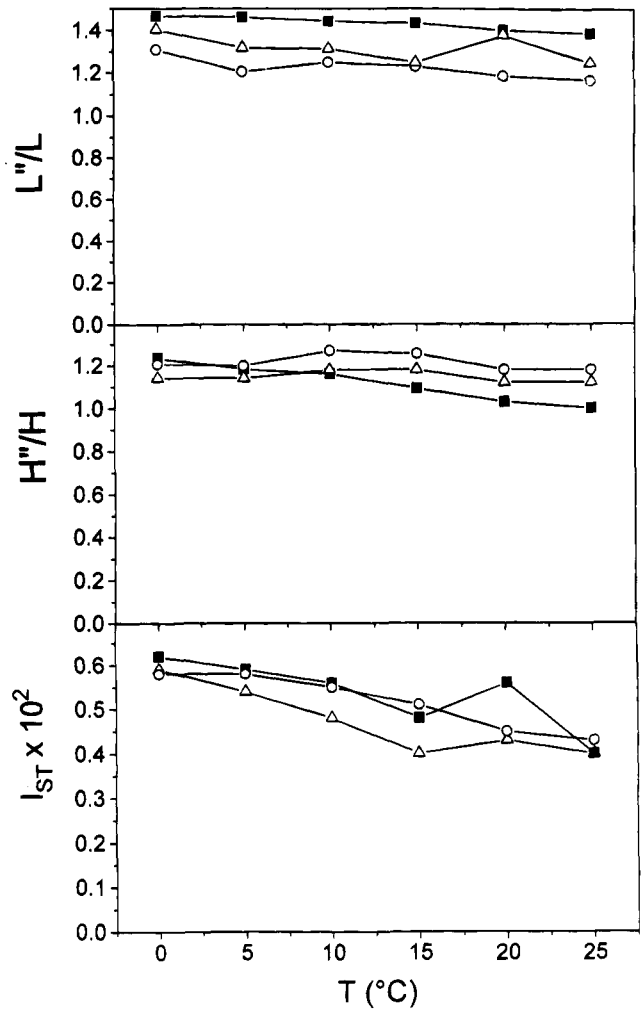

FIGURE 8: Temperature dependence of the STEPR spectral lineheight ratios from the low-field (L''/L) and high-field (H''/H) diagnostic regions and the normalized spectral integral ($I_{ST} \times 10^2$), for TITC labeled H/K-ATPase. The enzyme medium contained either 2 mM Mg^{2+} (△), 2 mM $MgSO_4$ and 2 mM ATP (■), or 2 mM $MgSO_4$, 2 mM ATP, and 1 mM SCH 28080 (○).

precably in the diagnostic regions by points of inflection associated with weakly constrained spin-label (on the conventional EPR time scale), which have complicated the analysis of spectra of spin-labeled Na/K-ATPase (Esmann et al., 1987, 1992). Rather, the major obstacle to quantitative analysis of the spectra was the presence of the two overlapping (S1 and S2) components from the strongly constrained labels (on the conventional EPR time scale). These could give rise to artifactual intensity in the diagnostic regions and lead to overestimation of the rotational correlation times based on this method.

In each of the series of STEPR spectra (Figure 7a–c), few overall changes in the spectral lineshapes were seen as the temperature was raised. This was illustrated quantitatively by the small changes in the diagnostic lineheight ratios, L''/L and particularly H''/H (Figure 8; Table 4). The values of lineheight ratios implied that enzyme rotation occurred on the STEPR time scale (Thomas et al., 1976; Hemminga & De Jager, 1989; Horváth & Marsh, 1988). It would be expected, therefore, that changes in lineshape occur with increasing temperature, reflecting increasing rotational diffusion of the enzyme. The low temperature dependence of

Table 4: STEPR Parameters for Gastric H/K-ATPase Covalently Labeled at Lysine Groups with TITC[a]

		lineheight ratio		
enzyme medium	temp (°C)	L''/L	H''/H	I_{ST} ($\times 10^2$)
control (1 mM EDTA)	0	1.40 (138)	1.14 (93)	0.59 (13)
	25	1.25 (81)	1.10 (89)	0.40 (2)
2 mM ATP	0	1.48 (169)	1.25 (123)	0.62 (19)
	25	1.38 (131)	1.00 (59)	0.40 (2)
1 mM SCH 28080	0	1.30 (100)	1.22 (115)	0.58 (13)
	25	1.17 (61)	1.19 (104)	0.43 (3)

[a] Effective rotational correlation times (τ_R^{eff}) were estimated from calibrations for isotropically tumbling spin-labeled hemoglobin (Horváth & Marsh, 1988) by numerical interpolation of lineheight ratios (L''/L, H''/H) and normalized integrals (I_{ST}). Uniaxial rotational correlation times, τ_{RII} (in microseconds, in parentheses), accounting for anisotropic motion of the enzyme were calculated from eq 1 assuming a perpendicular ($\theta = 90°$) orientation of the nitroxide z axis with respect to the axis of rotation.

L''/L and H''/H could be a corollary of the redistributing proportions of the two strongly constrained spin-label populations, which countered the changes in lineshape normally associated with increasing mobility. Normalized STEPR spectral integrals I_{ST} exhibited a steeper temperature dependence than did the corresponding lineheight ratios

(Figure 8, bottom panel). The progressive decline of I_{ST} was more reminiscent of increasing enzyme rotational mobility as the temperature was raised, suggesting that integrals were influenced less by the presence of two spin-label populations than were the lineheight ratios.

Enzyme uniaxial rotational correlation times were estimated from L''/L, H''/H, and I_{ST} at 0 °C (Table 4). At 0 °C, conventional EPR spectra exhibited predominantly a single outer (S2) component accounting for 84% of integrated intensity. Isotropic rotational correlation times τ_R^{eff} at 0 °C were determined using calibration plots for spin-labeled hemoglobin (Horvath & Marsh, 1988) and corrected for uniaxial, anisotropic rotation of the enzyme according to eq 2. This approach is only sufficient for estimating an upper limit of the uniaxial correlation time $\tau_{R||}$, because it assumes that all nitroxide z axes are perpendicular to the enzyme principal rotation axis, i.e., $\theta = 90°$ (Esmann et al., 1987). At 0 °C in the presence of the different ionic ligands, maximum enzyme rotational correlation times of 169 and 123 μs were determined from the values of L''/L and H''/H, respectively, compared to 13 μs measured from I_{ST} (Table 4). Although differences were observed in $\tau_{R||}$ for enzyme in the presence of the different ionic ligands, these were not large enough to represent significant changes in the rotational diffusion of the enzyme accompanying its conformational transitions.

The uniaxial rotational correlation time of H/K-ATPase can be used to estimate the intramembranous diameter of the enzyme according to hydrodynamic theory (e.g., Marsh & Horváth, 1989):

$$\tau_{R||} = 2\pi\eta a^2 h/3kT \quad (3)$$

where a is the intramembranous radius. Taking the upper limit correlation time to be 169 μs at 0 °C (determined from L''/L), and assuming membrane viscosity $\eta = 5$ P (Esmann et al., 1987) and membrane thickness $h = 4.5$ nm, yields an upper estimate radius of 108 Å for the intramembranous section of the enzyme, assuming $\theta = 90°$. A correlation time of 13 μs at 0 °C, as estimated using normalized integrals, yields a radius of 30 Å. The Stokes radii of $\alpha\beta$ or $\alpha_2\beta_2$ protomeric assemblies of detergent solubilized Na/K-ATPase are 66.4 and 77.4 Å, respectively (Esmann et al., 1987). Assuming that the dimensions of gastric H/K-ATPase α and β subunits are similar to those of Na/K-ATPase, our upper limit enzyme radius of 108 Å is somewhat larger than would be expected for the proposed $\alpha\beta$ promoter of H/K-ATPase. Conversely, the 30 Å (upper limit) radius measured from the normalized integrals is too low to account for even an $\alpha\beta$ promoter. This latter value must clearly be an underestimation, since many independent workers using different techniques have found that functional H/K-ATPase exists as an association of units. It is likely, then, that the true enzyme radius falls between these two values. Without eliminating uncertainties in the orientations of the spin-labeles and the possible lineshape distortions by the two overlapping components (e.g., by single site labeling), we refrain from drawing further conclusions on the dimensions of the enzyme at this stage.

CONCLUSIONS

It has long been a goal of workers in the field to establish the precise relationship between conformational changes of the H/K-ATPase and the mechanism by which the enzyme pumps protons into the stomach lumen. Advances in this regard have been made using spectroscopically receptive probes to visualize conformational transitions of the enzyme in terms of changes in the physicochemical properties of the probe (Jackson et al., 1983; Helmich-de Jong, 1987; Faller et al., 1991). A major problem with this approach has proved to be the inactivation of the ATPase function by derivatization, so that only ion sensitivity and partial reactions could be examined rather than the reaction cycle in its integrity (Jackson et al., 1983). For example, the fluorescent probe FITC specifically modifies a single lysine residue of the P-type ATPases with ensuing rapid and irreversible inactivation of ATP hydrolysis, probably because of steric interference of the bulky fluorescent probe with nucleotide binding (Karlish, 1980; Farley & Faller, 1985). Here, in contrast to FITC, spin-labeling of H/K-ATPase with TITC, which is also reactive toward the primary amine functionality of lysine residues, resulted in a uniform 35% reduction in rate of the control Mg^{2+} dependent and K^+ stimulated ATPase activity (Figure 2). This finding made it possible to examine the *functional* spin-labeled enzyme by EPR spectroscopy.

The conventional EPR spectrum of functional TITC labeled H/K-ATPase exhibited two distinct components, which probably represented two populations of spin-labels, strongly constrained by the enzyme but differing in their degrees of residual motional freedom. In previous work, it was found that ionic ligands induced conformational transitions of the H/K-ATPase, as deduced from transient changes in fluorescence of covalently attached probes or trypsin fragmentation patterns on SDS gels (Faller et al., 1991; Helmich-de Jong et al., 1988). In this work, we observed changes in the proportions of the two EPR spectral components with temperature, which were modulated by the presence of ionic ligands or the reversible inhibitor SCH 28080, suggesting that the spin-label environments are altered by conformational changes of the enzyme. Although at this stage one can only speculate what these changes mean precisely, we have demonstrated that EPR is a valuable tool for visualizing conformational transitions of H/K-ATPase.

ACKNOWLEDGMENT

The authors wish to thank Mr. Peter Fisher for his assistance with protein purification. We are also grateful to Dr. Andy Pope and Dr. Jeremy Rowntree for helpful advice and discussions.

REFERENCES

Chang, H., Saccomani, G., Rabon, E., Schackmann, R., & Sachs, G. (1979) *Biochim. Biophys. Acta 464*, 313−327.
Esmann, M. (1982) *Biochim. Biophys. Acta 688*, 251−259.
Esmann, M., Horváth, L. I., & Marsh, D. (1987) *Biochemistry 26*, 8675−8683.
Esmann, M., Hankovsky, H. O., Hideg, K., & Marsh, D. (1989) *Biochim. Biophys. Acta 978*, 209−215.
Esmann, M., Hideg, K., & Marsh, D. (1992) *Biochim. Biophys. Acta 1159*, 51−59.
Esmann, M., Karlish, S. J. D., Sottrup-Jensen, L., & Marsh, D. (1994) *Biochemistry 33*, 8044−8050.
Faller, L. D., Diaz, R. A., Scheiner-Bobis, G., & Farley, R. A. (1991) *Biochemistry 30*, 3503−3510.
Farley, R. A., & Faller, L. D. (1985) *J. Biol. Chem. 260*, 3899−3901.
Freed, J. H. (1976) in *Spin Labeling: Theory and Applications* (Berliner, L. J., Ed.) pp 53−161, Academic Press, New York.

Helmich-de Jong, M. L., van Duynhoven, J. P. M., Schuurmans Stekhoven, F. M. A. H., & de Pont, J. J. H. H. M. (1986) *Biochim. Biophys. Acta 858*, 254−262.
Helmich-de Jong, M. L., van Emst-de Vries, S. E., & de Pont, J. J. H. H. M. (1987) *Biochim. Biophys. Acta 905*, 358−370.
Hemminga, M. A., & de Jager, P. A. (1989) in *Spin Labeling: Theory and Applications* (Berliner, L. J., & Reuben, J., Eds.) pp 131−178, Plenum Press, New York and London.
Hemminga, M. A., de Jager, P. A., Marsh, D., & Fajer, P. (1984) *J. Magn. Reson. 59*, 160−163.
Hidalgo, C., Thomas, D. D., & Ikemoto, N. (1978) *J. Biol. Chem. 253*, 6878−6887.
Horváth, L. I., & Marsh, D. (1983) *J. Magn. Reson. 54*, 363−373.
Horváth, L. I., & Marsh, D. (1988) *J. Magn. Reson. 80*, 314−317.
Jackson, R. J., Mendlein, J., & Sachs, G. (1983) *Biochim. Biophys. Acta 731*, 9−15.
Karlish, S. J. D. (1980) *J. Bioenerg. Biomembr. 12*, 111−135.
Karon, B. S., & Thomas, D. D. (1993) *Biochemistry 32*, 7503−7511.
Keeling, D. J., Laing, S. M., & Senn-Bilfinger, J. (1988) *Biochem. Pharmacol. 37*, 2231−2236.
Keeling, D. J., Taylor, A. G., & Schudt, C. (1989) *J. Biol. Chem. 264*, 5545−5551.
Mendlein, J., & Sachs, G. (1990) *J. Biol. Chem. 265*, 5030−5036.
Rabon, E. C., & Reuben, M. A. (1990) *Annu. Rev. Physiol. 52*, 321−344.
Saccomani, G., Stewart, H. B., Shaw, D., Lewin, M., & Sachs, G. (1977) *Biochim. Biophys. Acta 465*, 311−330.
Sachs, G., Carlsson, E., Lindberg, P., & Wallmark, B. (1988) *Annu. Rev. Pharmacol. Toxicol. 28*, 269−284.
Sachs, G., Munson, K., Balaji, V. N., Aures-Fischer, D., Hersey, S. J., & Hall, K. (1989) *J. Bioenerg. Biomembr. 21*, 573−588.
Sachs, G., Besancon, M., Shin, J. M., Mercier, F., Munson, K., & Hersey, S. (1992) *J. Bioenerg. Biomembr. 24*, 301−308.
Swarts, H. G. P., van Uem, T. J. F., Hoving, S., Fransen, J. A. M., & de Pont, J. J. H. H. M. (1991) *Biochim. Biophys. Acta 1070*, 283−292.
Thomas, D. D., & Hidalgo, C. (1978) *Proc. Natl. Acad. Sci. U.S.A. 75*, 5488−5492.
Thomas, D. D., Dalton, L. R., & Hyde, J. S. (1976) *J. Chem. Phys. 65*, 3006−3024.
Van der Hijden, H. T. W. M., Koster, H. P. G., Swarts, H. P. G., & de Pont, J. J. H. H. M. (1990) *Biochem. J. 267*, 565−572.
Wallmark, B., Briving, C., Fryklund, J., Munson, K., Jackson, R., Mendlein, J., Rabon, E., & Sachs, G. (1987) *J. Biol. Chem. 262*, 2077−2084.

BI9422485